JOURNAL OF VIROLOGY, Jan. 2011, p. 217–230 Vol. 85, No. 1
0022-538X/11/$12.00 doi:10.1128/JVI.01805-10

Successful Vaccination Strategies That Protect Aged Mice from Lethal Challenge from Influenza Virus and Heterologous Severe Acute Respiratory Syndrome Coronavirus▽

Timothy Sheahan,[1,3] Alan Whitmore,[2] Kristin Long,[2] Martin Ferris,[2] Barry Rockx,[3,6] William Funkhouser,[4] Eric Donaldson,[3] Lisa Gralinski,[3] Martha Collier,[2] Mark Heise,[1,2,5] Nancy Davis,[1,2] Robert Johnston,[1,2] and Ralph S. Baric[1,3]*

Department of Microbiology and Immunology, University of North Carolina at Chapel Hill, Chapel Hill, North Carolina[1]; Carolina Vaccine Institute, University of North Carolina at Chapel Hill, Chapel Hill, North Carolina[2]; Department of Epidemiology, University of North Carolina at Chapel Hill, Chapel Hill, North Carolina[3]; Department of Pathology, University of North Carolina School of Medicine, Chapel Hill, North Carolina[4]; Department of Genetics, University of North Carolina at Chapel Hill, Chapel Hill, North Carolina[5]; and Laboratory of Virology, Rocky Mountain Laboratories, National Institute of Allergy and Infectious Diseases, National Institutes of Health, Hamilton, Montana[6]

Received 26 August 2010/Accepted 19 October 2010

Newly emerging viruses often circulate as a heterogeneous swarm in wild animal reservoirs prior to their emergence in humans, and their antigenic identities are often unknown until an outbreak situation. The newly emerging severe acute respiratory syndrome coronavirus (SARS-CoV) and reemerging influenza virus cause disproportionate disease in the aged, who are also notoriously difficult to successfully vaccinate, likely due to immunosenescence. To protect against future emerging strains, vaccine platforms should induce broad cross-reactive immunity that is sufficient to protect from homologous and heterologous challenge in all ages. From initial studies, we hypothesized that attenuated Venezuelan equine encephalitis virus (VEE) replicon particle (VRP) vaccine glycoproteins mediated vaccine failure in the aged. We then compared the efficacies of vaccines bearing attenuated (VRP_{3014}) or wild-type VEE glycoproteins (VRP_{3000}) in young and aged mice within novel models of severe SARS-CoV pathogenesis. Aged animals receiving VRP_{3000}-based vaccines were protected from SARS-CoV disease, while animals receiving the VRP_{3014}-based vaccines were not. The superior protection for the aged observed with VRP_{3000}-based vaccines was confirmed in a lethal influenza virus challenge model. While the VRP_{3000} vaccine's immune responses in the aged were sufficient to protect against lethal homologous and heterologous challenge, our data suggest that innate defects within the VRP_{3014} platform mediate vaccine failure. Exploration into the mechanism(s) of successful vaccination in the immunosenescent should aid in the development of successful vaccine strategies for other viral diseases disproportionately affecting the elderly, like West Nile virus, influenza virus, norovirus, or other emerging viruses of the future.

Newly emerging and reemerging viruses often circulate as a heterogeneous swarm in wild animal reservoirs prior to their emergence into the human population, and thus their antigenic identities are often unknown until outbreak situations. Although design of a vaccine that is protective against both contemporary and future emergent strains can be challenging, this conundrum may in part be deflected through the development vaccines that induce broad cross-reactive immunity, increasing the likelihood of the protection from future emergent strains. The newly emerging severe acute respiratory syndrome coronavirus (SARS-CoV) and the reemerging influenza virus exemplify the many difficulties associated with effective vaccine design for emerging pathogens. SARS-CoV emerged suddenly in Guangdong Province in China in 2002 and reemerged in 2004, causing over 8,000 cases and greater than 700 deaths in 29 countries throughout the world (42). Recently, zoonotic ancestors to the epidemic strain (SARS Urbani) have been found in the putative animal reservoir, the Chinese horseshoe bat, as well as in other exotic species commonly sold for food, like raccoons, dogs, and palm civets (33). SARS-CoV disease is characterized by an atypical pneumonia, in which approximately 20% of cases progressed to a particularly devastating and clinically challenging end-stage disease, acute respiratory distress syndrome (ARDS), requiring admission to intensive care and mechanical ventilation (12, 34, 36, 45, 46). SARS-CoV disease severity was directly associated with increasing age, as mortality rates in people over the age of 65 exceeded 50% (16, 29). Currently, a vaccine is not available for SARS-CoV. Similar to SARS-CoV, influenza virus causes disproportionate disease in the elderly; 90% of influenza-related deaths in the United States (~36,000/year) occur in people over the age of 65 (41, 61). Although a seasonal influenza vaccine is available, its efficacy is diminished in the most vulnerable aged populations (17 to 53% effectiveness in the elderly, 70 to 90% effectiveness in young adults) (25). Further complicating influenza vaccine development are the phenomena of antigenic drift and the antigenic shift most recently seen by the rapid and unexpected emergence of pandemic H1N1 influenza virus in 2009, in which the previous 30 years of seasonal influenza

* Corresponding author. Mailing address: Department of Epidemiology, 2107 McGavran-Greenberg, CB7435, University of North Carolina, Chapel Hill, NC 27699-7435. Phone: (919) 966-3895. Fax: (919) 966-2089. E-mail: rbaric@email.unc.edu.

▽ Published ahead of print on 27 October 2010.

vaccines afforded little protection against the newly emerged pandemic strain (30). Lastly, two of the recently emerged influenza viruses, H5N1 and H1N1, caused a severe ARDS-like disease similar to the severe cases of SARS-CoV (40, 70). Given the global public health impacts of both SARS-CoV and influenza virus, the development of vaccine platforms that induce broadly cross-reactive immune responses in all age groups is highly desirable.

The successful vaccination of elderly populations is a difficult and unpredictable task due to deficiencies in the immune system that develop with aging (9, 10, 19, 21, 25–27, 31, 44, 62, 63). Immunosenescence, the gradual deterioration of the immune system that occurs gradually with age, affects the innate and adaptive immune compartments, contributing to decreased vaccine efficacy in the aged (19, 21, 24–26, 31, 39, 62, 64). For example, defects in antigen presentation, T cell activation, and cytokine secretion affect the generation of effective adaptive immune system helper cells (T helper or Th cells) and effector cells (B cells and cytotoxic T cells), resulting in diminished vaccine efficacy(19, 20, 24–26, 31, 39, 62, 64). Although both SARS-CoV and influenza virus cause more severe disease in the aged, few vaccine studies for SARS-CoV and influenza virus have been performed in aged mouse models and even fewer have been evaluated through heterologous virus challenge, which mimics vaccine challenge by divergent newly emerging strains (3, 6, 15, 32, 66). Venezuelan equine encephalitis virus (VEE) replicon particle (VRP) vaccines have recently been clinically proven to be safe, replication-incompetent vaccine vectors capable of inducing mucosal immunity from a peripheral route of inoculation (8, 37, 60). To create a VRP, the region of the genome encoding the viral glycoproteins is replaced with a transgene of interest, and to "package" this chimeric RNA, VEE glycoproteins are provided in *trans*. To date, VRP vaccines for human use and our previous SARS-CoV vaccine studies have employed attenuated "traditional" VEE coat proteins from the attenuated VEE 3014 strain (VRP_{3014}). The rationale for using attenuated glycoproteins was to ensure there were several mechanisms of attenuation within the vaccine vector, thereby enhancing safety. Compared to wild-type VEE 3000, the VEE 3014 strain differs by only 3 amino acids within the viral glycoproteins, which have been demonstrated to completely abrogate virus-induced mortality through alteration of *in vivo* cell targeting (7, 38). In 2003, Deming et al. demonstrated that vaccination with VRP assembled with VEE 3014 strain coat proteins expressing SARS Urbani S (VRP-S) provided complete protection from virus replication in young mice but limited protection in aged mice after heterologous challenge (icGD03-S), and protection was coincident with the development of neutralizing antibodies (15). Since the SARS-CoV replication models lack notable morbidity and mortality, all earlier studies were unable to assess protection from severe disease/death, and those investigators could only speculate that diminishing virus replication might result in reduced disease severity (15, 50, 59).

Using divergent SARS-CoV strains rMA15 and rMA15 GD03-S, we developed two novel BALB/c mouse models of SARS-CoV pathogenesis with age-dependent morbidity/mortality and pathological findings of acute ARDS similar to those noted in fatal human infections. Within these models of SARS-CoV pathogenesis, we demonstrated that multiple antigenically divergent VRP_{3014}-based VRP vaccines failed to protect against replication, disease, and mortality following lethal homologous and heterologous SARS-CoV challenge in aged mice. Given the failure of VRP_{3014}-based vaccines in the aged, we sought to compare the efficacy of VRP_{3014}- and VRP_{3000}-based vaccines in young and aged animals with both lethal homologous (SARS-CoV/influenza virus) and heterologous (SARS-CoV) challenge. Importantly, aged animals that received the VRP_{3000}-based vaccines were completely protected from influenza virus-induced morbidity and mortality, while near-complete protection from homologous and heterologous SARS-CoV challenge was achieved. Protection from mortality in aged animals was coincident with the generation of neutralizing antibody. These data suggest that the specifications of the VRP vaccine platform are key for the successful vaccination of aged populations, who are more vulnerable to severe disease caused by SARS-CoV and influenza virus. Future studies with the VRP vaccine platform should provide further insight into the mechanisms of successful protection in the elderly, and this technology could be adapted to target other diseases that cause disproportionate disease in the elderly, like West Nile virus, norovirus, and other emerging viral diseases in the future.

MATERIALS AND METHODS

Viruses and cells. For the recombinant epidemic virus strain icSARS (AY278741), rMA15, icGD03-S (AY525636), and rMA15 GD03-S, titers were determined and viruses were propagated on Vero E6 cells as described elsewhere (68). Vero E6 cells were grown in minimal essential medium (Invitrogen, Carlsbad, CA) supplemented with 10% FCII (HyClone, South Logan, UT) and gentamicin-kanamycin (UNC Tissue Culture Facility). All SARS-CoV virus work was performed in a class II biological safety cabinet in a certified biosafety level 3 laboratory containing redundant exhaust fans, with laboratory personnel wearing Tyvek suits and powered air-purifying respirators as described previously (69). Recombinant influenza virus PR8 strain stock was kindly donated by Peter Palese at Mt. Sinai Medical Center in New York City. All influenza virus work was performed in a class II biological safety cabinet in a biosafety level 2 laboratory.

Construction of rMA15 GD03-S. rMA15 differs from the epidemic strain SARS Urbani by 6 amino acids (H133Y nsp5, E269A nsp5, T67A nsp9, A4V nsp13, Y436H Spike, and E11K M). Recently, we introduced the GD03-S glycoprotein into the SARS Urbani infectious clone, which resulted in the creation of a recombinant chimeric SARS-CoV bearing a GD03-S, but this virus did not produce lethal disease or cause significant weight loss in young or aged animals (15, 53). To construct a recombinant mouse-adapted SARS-CoV bearing the most divergent human SARS-CoV spike (S) glycoprotein, we inserted the GD03 spike gene (GenBank accession no. AY525636) into our infectious cDNA clone of mouse-adapted SARS-CoV (rMA15) while retaining the mouse-adapting S mutation Y436H (49). The SARS-CoV infectious cDNA clone was split among six plasmids (A to F), and the S gene was split among the E and F plasmid clones. The Y436H mutation was introduced into the GD03-S sequence by using overlapping PCR. Briefly, the icSARS-GD03-E pSMART fragment DNA was amplified by PCR using Expand high-fidelity polymerase (Roche, Indianapolis, IN) with the following primer sets: amplicon A (NcoIF, 5′-TGTTTCTAAACCCAT GGGTACACAG-3′; MA15spkR, 5′-GATACCTATATTTATAATTATGATT ACCAG-3′) and Amplicon B(XbaIR, 5′-GGGCCCTCTAGAGATCGAGC-3′; MA15spkF, 5′-CTGGTAATCATAATTATAAATATAGGTATC-3′). The final overlap amplicon was purified using a Qiagen (Valencia, CA) PCR purification kit and digested with NcoI and XbaI (New England BioLabs [NEB], Ipswich, MA) for 1 h at 37°C. The target vector, icSARS GD03-E pSMART, was digested similarly. The digested overlap amplicon (2.2 kb) and vector fragments (5.3 kb) were gel purified using a QIAquick gel purification kit (Qiagen), ligated to create rMA15 GD03-E pSMART, and sequence verified. To generate rMA15 GD03-F pSMART, the 5′ end of the GD03 spike contained in the icSARS GD03-F plasmid was shuttled into the rMA15 F TOPO-XL plasmid. icSARS GD03 F pSMART was digested with BamHI (NEB), while rMA15-F TOPO-XL was digested with BamHI and CIP (NEB). icSARS-GD03-F pSMART (2,059 bp) and rMA15-F TOPO-XL (7,260 bp) fragments were gel purified and ligated to

create rMA15 GD03-F TOPO-XL. Full-length rMA15 GD03-S cDNA was constructed, and *in vitro* transcripts were generated and electroporated into Vero E6 cells to create recombinant virus as described elsewhere (68). The rMA15 GD03-S virus from electroporation was passaged until cytopathic effect (CPE) was seen (two passages) and plaque purified, and plaques were expanded on Vero E6 cells to create a working virus stock, which was stored at −80°C until use. Viral RNA from the rMA15 GD03-S virus stock was isolated using TRIzol (Invitrogen), cDNA was synthesized using SuperScript II (Invitrogen), and regions spanning the S, 3a, E, and M genes were PCR amplified and directly sequenced. All GD03-S mutations and the Y436H mutation were present, but one additional coding change was found outside the receptor binding domain of S at residue 623, resulting in a change from serine to tyrosine.

The nucleotide sequences for the SARS variants used in this study have the following GenBank accession numbers: SARS-CoV Urbani, AY278741; SZ16, AY304488; GD03, AY525636). The influenza virus PR8 (A/Puerto Rico/8/34) genes are catalogued as follows: PB2, GI 60484; PB1, GI 324897; PA, GI 60808; HA, GI 62290; NP, GI 324709; NA, GI 324507; M, GI 60788; NS, GI 324833.

Virus growth curve analysis. Vero E6 cells were infected with icSARS, icGD03-S, rMA15, or rMA15 GD03-S at a multiplicity of infection (MOI) of 0.01 for 1 h at 37°C, after which the inoculum was removed, the monolayer was rinsed with Dulbecco's phosphate-buffered saline (DPBS), and growth medium was added. Medium was sampled at 0, 6, 12, 24, and 36 h postinfection (hpi), and samples were stored at −80°C until titers were determined by plaque assay in Vero E6 cells as described elsewhere (68).

Infection of young and aged BALB/c mice with SARS-CoV. Animal housing and care were in accordance with all University of North Carolina Institutional Animal Care and Use Committee guidelines. All BALB/c mice were purchased from Harlan Sprague Dawley (Indianapolis, IN). Ketamine-anesthetized 10-week-old (n = 10/virus) or 12-month-old (n = 6/virus) female BALB/c mice were intranasally infected with 10^5 PFU of rMA15 or rMA15 GD03-S in 50 μl, after which clinical signs of disease (body weight) were monitored every day postinfection. At 2 and 4 days postinfection (dpi), groups of animals were sacrificed and lungs were removed for histology and virus lung titer determinations using the methods described below.

Lethal SARS-CoV challenge of aged BALB/c mice vaccinated with traditional VRP-expressing Urbani S, GD03-S, SZ16-S, a pool of all three S-expressing VRPs, or influenza virus HA. Twelve-month-old female Harlan Sprague Dawley BALB/c mice (Indianapolis, IN) were vaccinated with 10^5 infectious units (IU)/10 μl of either influenza virus hemagglutinin (HA) glycoprotein, SARS-S, GD03-S, SZ16-S VRP, or a pool of SARS S containing VRPs (pool-S; 10^5 IU/antigen) in the left rear footpad. The SARS-CoV strain GD03 was isolated from a patient in the Guangdong region in China during the reemergence of 2003–2004, and it clusters with zoonotic viruses that were isolated from civets in live animal markets during those outbreaks (15, 28, 53, 55, 56). SARS-CoV SZ16 was isolated from a Himlayan palm civet, and its S protein differs from the epidemic strain, SARS-CoV Urbani, in 18 amino acids (13, 28, 55, 56). All VRPs were "packaged" with VEE_{3014} strain glycoproteins (7, 14, 47). VRP IU titers were generated through infection of baby hamster kidney (BHK) cells as described elsewhere (22). Three weeks after primary vaccination ("prime"), animals were bled to assess SARS S-specific serum IgG. At 13 months of age, mice received a secondary vaccination ("boost") of the same dose and identity of their primary vaccination. At 15 months of age, mice were bled to assess postboost SARS-CoV-S-specific serum IgG and neutralizing antibody. A week later, mice were intranasally infected with 10^5 PFU/50 μl rMA15 GD03-S. Mice were monitored daily for clinical signs (weight) and mortality. At 2 dpi, when SARS-CoV lung titers are maximal, three animals per group were sacrificed to assess virus lung titer and histology as described below. In an additional experiment, 12-month-old female BALB/c mice were vaccinated with 10^6 IU of VRP Urbani-S in a similar prime/boost regimen as described above. Prior to challenge, sera were taken to measure the antigen-specific IgG response. At 17 months of age, animals were intranasally infected with 10^5 PFU/50 μl rMA15-GD03-S, after which morbidity and mortality were monitored.

Vaccination and lethal SARS-CoV challenge of young adult and aged BALB/c mice with VRPs packaged with wild-type VEE 3000 strain or traditional 3014 strain glycoproteins. Young adult and aged BALB/c mice were vaccinated with VRPs expressing SARS-CoV GD03-S antigen packaged with either VRP_{3000} or VRP_{3014} glycoproteins. Young adult and aged mice were vaccinated and boosted with 10^5 IU of VRP_{3000} GD03-S or VRP_{3014} GD03-S. Young adult mice (VRP_{3000} GD03-S, n = 15; VRP_{3014} GD03-S, n = 18) received their primary vaccination at 8 weeks of age and were boosted at 11 weeks of age. Aged mice (VRP_{3000} GD03-S, n = 16; VRP_{3014} GD03-S, n = 14) received their primary vaccination at 12 months of age and were boosted at 13 months of age. All mice were bled 2 weeks post-prime/boost in order to assess antigen-specific immune responses by an enzyme-linked immunosorbent assay (ELISA) and neutralization assay. At 14 weeks of age, young adult mice groups were each divided in half, with one half receiving intranasal homologous challenge (10^5 PFU rMA15 GD03-S) and the other half receiving a heterologous challenge (10^5 PFU rMA15). Groups of aged mice were divided into half and challenged similarly to the young groups as described above. After challenge, mice were monitored daily for morbidity (weight) and mortality. At 2 dpi, three mice in each group were sacrificed and lungs were harvested for virus titer determinations and pathology as described below. In the experiments above, equivalent PFU of VRP_{3000} and VRP_{3014} were delivered. In an additional experiment to assess the magnitude of the SARS-S-specific immune responses in young and aged animals after vaccination with equivalent genomes of VRP_{3000} and VRP_{3014}, 1.4×10^6 genomes of either VRP_{3000} GD03-S or VRP_{3014} GD03-S were administered in a prime/boost regimen in BALB/c mice similar in age and sex to those above (n = 6 to 7 mice/group).

Vaccination and lethal influenza virus challenge of young adult and aged BALB/c mice with VRPs packaged with wild-type VEE 3000 strain or traditional 3014 strain glycoproteins. Similar to the SARS-CoV experiment described above, VPR vaccines expressing the chief influenza virus protective antigen, HA (strain PR8), were generated with either VEE 3000 or VEE 3014 coat proteins. Young adult and aged mice were vaccinated and boosted with 10^5 IU of VRP_{3000} HA or VRP_{3014} HA. Young adult mice (VRP_{3000} HA, n = 9; VRP_{3014} HA, n = 9) received their primary vaccination at 8 weeks of age and were boosted at 11 weeks of age. Aged mice (VRP_{3000} HA, n = 7; VRP_{3014} HA, n = 9) received their primary vaccination at 12 months of age and were boosted at 13 months of age. To assess antigen-specific immune responses prior to challenge, serum from all mice was collected 2 weeks post-prime/boost and analyzed by ELISA and hemagglutination inhibition assay. At 14 weeks (young adult) and 15 months (aged), mice were challenged with 500 PFU (~10 50% lethal doses) of influenza virus PR8. To demonstrate the pathogenesis of PR8 in unvaccinated young and aged mice, we infected age-matched (14 weeks or 12 to 15 months) and sex-matched unvaccinated BALB/c mice at the time of vaccine challenge. After virus challenge, morbidity (weight) and mortality were monitored daily. On day 3 pi, three mice in each group were sacrificed and lungs were harvested for virus titer determinations and pathology as described below.

ELISA to assess SARS S-specific IgG in mouse sera. Antibodies directed against SARS S antigen were quantitated in an ELISA as previously described (4, 15). Antigens for the ELISA were purchased (purified recombinant SARS Urbani S proteins; BEI Resources, Manassas, VA) or generated through infection of BHK cells with VRP GD03-S, VRP SZ16-S, or VRP HA. When using cell lysates as antigen, a VRP expressing an irrelevant antigen in the ELISA was included to control for background associated with VRP-specific antibodies in vaccinated mice. Titers represent the serum dilution that corresponded to half the maximum absorbance for each sample, measured at 450 nm. Comparisons between half-maximal titers derived from different experimental groups were statistically evaluated using the Mann-Whitney test, a nonparametric method. Except for the "equivalent VRP genome" experiment described above, all sera used in ELISAs were obtained from vaccinated animals that were subsequently challenged.

Microneutralization and PRNT assays. For the microneutralization assay, heat-inactivated serum was serially diluted in 2-fold increments beginning at 1:25, mixed with 100 PFU of rMA15 GD03-S, and incubated for 1 h at 37°C. The combination of virus and serum was then added to a 96-well plate of Vero E6 cells (5×10^3 Vero E6 cells/well) in triplicate and incubated at 37°C until CPE was assessed (4 to 5 dpi). For each dilution of serum, the number of wells protected from CPE was scored. The greatest dilution of serum with more than two wells of protection was considered the 50% neutralization titer (52). For the plaque reduction neutralization (PRNT) assay, 100 PFU of rMA15 GD03-S was incubated with 1:2 dilutions of heat-inactivated sera (final concentrations of diluted sera ranged from 1:100 to 1:1,600) or medium (negative control) for 1 h at 37°C. After the incubation, the serum-virus and medium-virus cocktails were used as samples in a standard plaque assay. All serum samples were evaluated in duplicate. The relative percentage of plaque reduction due to neutralization was generated by comparing the average number of plaques per dilution of serum and the number of plaques generated in the negative-control samples (virus plus medium without serum). The dilution at which 50% of plaques were neutralized was considered our $PRNT_{50}$ value. All sera used in neutralization assays were obtained from vaccinated animals that were subsequently challenged.

Hemagglutination inhibition assay. For the hemagglutination inhibition (HAI) assay, a measurement of influenza virus HA-specific antibody responses and a correlate of protection, 4 hemagglutinating units (HAU) of influenza virus strain PR8 in 25 μl were mixed with 2-fold serial dilutions of animal serum (25 μl per dilution) and incubated at room temperature for 30 min. Fifty microliters

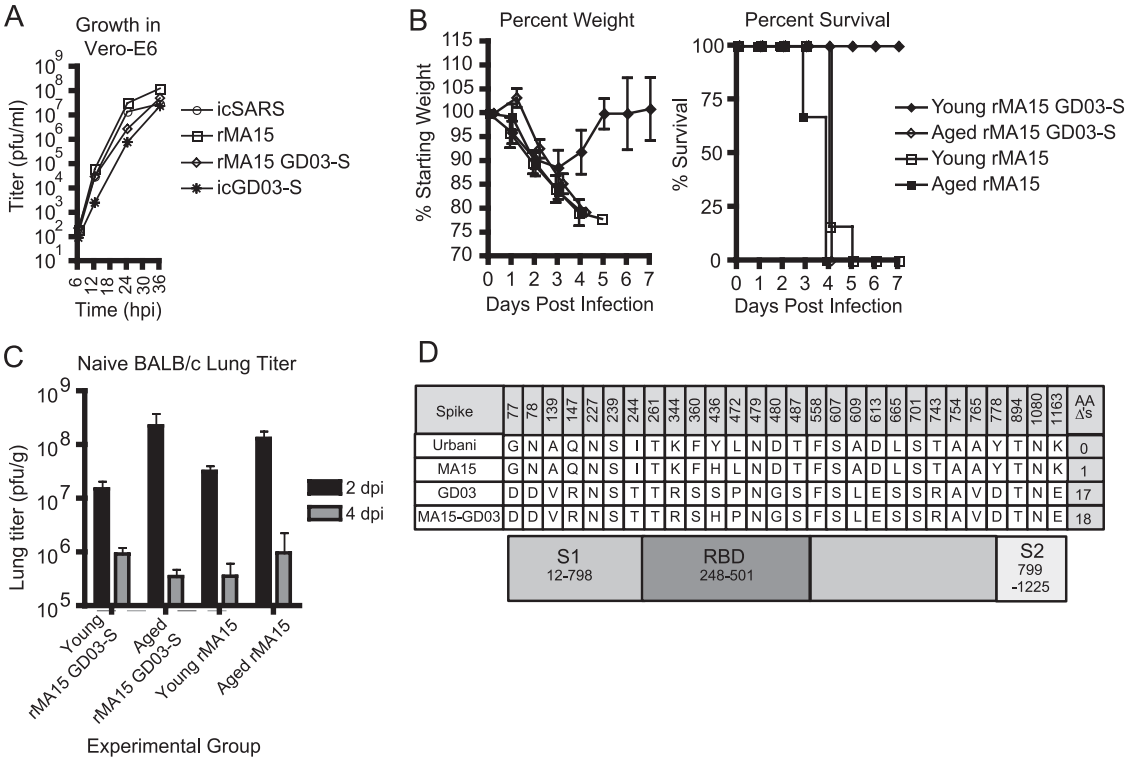

FIG. 1. *In vitro* and *in vivo* characterizations of rMA15 GD03-S. (A) Vero E6 cells were infected at an MOI of 0.01 with rMA15, icSARS, or rMA15 GD03-S for 1 h at 37°C, after which monolayers were rinsed with DPBS and growth medium was added. At various times postinfection, cell medium was sampled and frozen at −80°C until titers were determined by plaque assay in Vero E6 cells. (B) Ketamine-anesthetized 10-week-old (n = 10 animals/virus) or 12-month-old (n = 6 animals/virus) female BALB/c mice were infected with 10^5PFU/50 μl of rMA15 or rMA15 GD03-S, after which clinical signs of disease (weight loss) and mortality were monitored every day postinfection. Animals at or below 80% of the starting weight were sacrificed based on the IACUC protocol. On days 2 and 4 postinfection, groups of animals were sacrificed and lungs were removed for histology and virus lung titer determinations. Error bars represent 1 standard deviation. (C) Virus titers in the lungs of mice were measured by standard plaque assay in Vero E6 cells. Error bars represent 1 standard deviation. (D) Schematic of S amino acid changes comparing Urbani, GD03, MA15, and MA15 GD03-S.

of a 1% suspension of fresh chicken red blood cells (CRBCs) was then added to each well. In wells with anti-HA antibody, virus was bound by antibody and was not available to agglutinate the CRBCs. The maximal reciprocal serum dilution where agglutination was completely inhibited is reported as the HAI value. All sera used in the HAI assay were obtained from vaccinated animals that were subsequently challenged.

Plaque assay to assess SARS-CoV lung titer. For determination of SARS-CoV lung titers, briefly, portions of the lungs were weighed, placed in 0.5 ml DPBS, and frozen at −80°C until analyzed. Lungs were then homogenized in a Magnalyzer (Roche) and clarified by centrifugation (12,000 rpm; 1 min in a microcentrifuge), and virus titers within lung supernatants were assessed via plaque assay in Vero E6 cells as described elsewhere (56).

$TCID_{50}$ determinations to assess influenza virus lung titer. To quantitate the amount of virus replication in naïve and vaccinated animals infected with the lethal influenza virus strain PR8, we performed a 50% tissue culture infected dose ($TCID_{50}$) assay on clarified mouse lung homogenates according to methods previously described (48). At 24 h prior to the start of the assay, Madin-Darby canine kidney (MDCK) cells were plated in 96-well plates at a density of 10^5 cells/well. Twofold dilutions of clarified lung homogenates (see above) were added in duplicate to 96-well plates of MDCK cells and incubated at 37°C for 1 h, after which wells were rinsed and cell culture medium was added. As a positive assay control, the titer of a previously characterized PR8 stock was also assessed. After 3 days, cell culture medium was removed and plates were stained with a vital crystal violet stain. The $TCID_{50}$ titer/g was calculated as previously described (48).

Lung histology. Lungs were fixed in 4% paraformaldehyde (PFA), paraffin embedded, sectioned, and stained with hematoxylin and eosin (H&E). Sections were evaluated and scored blindly by a trained pathologist (W. Funkhouser) for levels of inflammation and lung tissue damage.

Statistical analysis. Statistical analysis was performed using the Prism software (GraphPad, San Diego, CA). Nonparametric Mann-Whitney tests were performed to generate the P values noted below in the text and figures.

Ethics statement. Experimental animal protocols were reviewed and approved by the Institutional Animal Care and Use Committee at UNC Chapel Hill according to guidelines set by the Association for the Assessment and Accreditation of Laboratory Animal Care (AAALAC) and the United States Department of Agriculture (USDA).

RESULTS

rMA15 GD03-S, rMA15, and epidemic SARS-CoV grow to similar peak titers *in vitro*. Compared to the epidemic strain, SARS Urbani, the mouse-adapted strain MA15 contains six amino acid changes, one of which resides within the spike gene (Fig. 1D). To mimic vaccine challenge by a newly emerged pathogenic SARS-CoV strain, we constructed a recombinant mouse-adapted SARS-CoV (rMA15-GD03-S) within the MA15 background bearing a modified S of the most divergent human strain, GD03 (i.e., native GD03-S, including the Y436H mouse-adapting mutation) (15, 28, 53, 55). The GD03 S glycoprotein differed from Urbani by 17 amino acids (Fig. 1D), and cross-neutralization of GD03 using antisera directed against Urbani-S was reduced 10- to 15-fold (15). One amino acid change relative to the cloned sequence (S623Y) was found

in the rMA15 GD03-S spike gene, possibly resulting from passage in culture while generating the virus stock. Interestingly, the recombinant icSARS GD03-S virus described by Deming et al. developed a mutation (D613G) in a similar region of S during the process of virus stock generation, suggesting that some unique selective advantage for growth in culture may be encoded within this undefined region of S (15). To assess virus growth kinetics *in vitro*, Vero E6 cells were infected with rMA15, rMA15 GD03-S, icGD03-S, or icSARS (recombinant epidemic strain) at an MOI of 0.01. At 12 hpi, rMA15, rMA15 GD03-S, and icSARS titers were 1 log higher than that of icGD03-S. Although icGD03-S and rMA15 GD03-S growth seemed to be depressed at 24 hpi, all viruses eventually achieved similar peak titers ($<10^8$ PFU/ml) at 36 hpi (Fig. 1A).

Age is a critical factor in development of ARDS in BALB/c mice infected with rMA15 GD03-S. Since the pathogenesis of MA15 had not yet been evaluated in aged mice, we evaluated the *in vivo* growth kinetics and pathogenesis of the novel rMA15 GD03-S and parent rMA15. Upon infection of 10-week-old BALB/c mice with 10^5 PFU of rMA15 GD03-S or rMA15, all rMA15 GD03-S-infected mice lost approximately 10% of their body weight but survived, while rMA15-infected mice rapidly lost 20% of their starting weight and uniformly succumbed to infection by 5 dpi (Fig. 1B). Interestingly, virus titers for rMA15 and rMA15 GD03-S were similar at both 2 dpi (rMA15, 3.2×10^7 PFU/g; rMA15 GD03-S, 1.5×10^7 PFU/g) and 4 dpi (rMA15, 3.6×10^5 PFU/g; rMA15 GD03-S, 9.3×10^5 PFU/g) (Fig. 1C). Unlike infection of young adult mice, infection of aged mice with rMA15 or rMA15 GD03 was uniformly lethal, causing rapid weight loss (~20% starting weight) and 100% mortality by 3 to 4 dpi (Fig. 1B).

To determine the severity and potential age-related differences in lung pathology, H&E-stained lung sections from mock-infected and SARS-CoV-infected mice (2 and 4 dpi) were blindly evaluated (Fig. 2). Compared to mock-infected animals at 2 dpi, young and aged animals infected with rMA15 or rMA15 GD03 experienced a denuding bronchiolitis with an accumulation of apoptotic debris within the airways and lymphocytic perivascular cuffing that was more severe in the aged. In contrast to young infected mice, the hallmarks of diffuse alveolar damage (DAD) and ARDS (i.e., hyaline membranes in the alveoli [Fig. 2, double-headed arrow]) were readily observed at 4 dpi in aged infected mice, suggesting that death was likely due to DAD/ARDS-mediated respiratory failure. These data demonstrate that rMA15 and rMA15 GD03-S infection causes age-related severe end-stage lung pathogenesis (ARDS) similar to what has been observed in the most severe human cases.

Vaccination of aged mice with traditional VRP expressing either Urbani-S, GD03-S, SZ16-S, or a cocktail of all three VRP-S vaccines does not enhance protection from morbidity or mortality. Since Deming et al. demonstrated that traditional VRP_{3014} vaccines fail in aged mice upon heterologous challenge in a replication model, we sought to investigate the efficacy of VRP_{3014} vaccines in aged mice through lethal SARS-CoV heterologous challenge (15). Moreover, we hypothesized that vaccination with a pool of divergent SARS-CoV S antigens would increase the breadth of the immune response in aged animals, providing increased protection from a lethal heterologous challenge compared to animals receiving a monovalent vaccination. To test this hypothesis we vaccinated 12-month-old female BALB/c mice in a prime/boost regimen with traditional VRP_{3014}-expressing SARS Urbani-S (epidemic strain), GD03-S (the most divergent human strain), SZ16-S (civet strain), a pool of all three SARS-CoV S antigens (pool-S), or a control VRP expressing the influenza virus HA glycoprotein. At 15 months of age, mice were intranasally challenged with 10^5 PFU of rMA15 GD03-S, after which morbidity and mortality were monitored daily. All groups exhibited significant morbidity (>20% loss of starting weight by 4 dpi) and mortality (70 to 100%) after rMA15 GD03-S infection (Fig. 3A). The groups receiving the VRP_{3014}-expressing Urbani-S, GD03-S, or pool-S demonstrated various degrees of survival, while 100% of VRP_{3014} HA-vaccinated and VRP_{3014} SZ16-S-vaccinated mice died (Fig. 3A). Groups receiving the homologous antigen (GD03-S or pool-S) demonstrated similar levels of protection, suggesting that the other pool-S antigens did not provide an additional protective benefit. Virus lung titers were similarly high at 2 dpi ($<10^8$ PFU mean lung titer) in all vaccine groups (Fig. 3B). To determine the degree of lung pathology at 2 dpi, H&E-stained lung sections were evaluated blindly (Fig. 3E). Peribronchivascular cuffing by lymphocytes and neutrophils was evident in all groups at low magnification (×40). Denuding bronchiolitis, focal apoptosis of the airway epithelium, and blockage of the airway with apoptotic debris were evident in GD03-vaccinated and pool-S-vaccinated animals, but these manifestations of disease were more prominent in Urbani-, SZ16-, and HA-vaccinated animals. Although virus titer data at 2 dpi were similar for all groups, the pathology and morbidity/mortality data suggest that animals receiving the GD03-S antigen (GD03-S or pool-S) experienced at best a very low level of protection from the most severe disease seen in the other groups. Importantly, increasing the dose of VRP_{3014} Urbani-S to 10^6 IU in a prime/boost regimen did not improve morbidity (weight nadir at 4 dpi, 85% ± 9%) (mean ± standard deviation) or mortality (50%) to a level of complete protection in aged mice following heterologous lethal challenge with rMA15 GD03-S, suggesting that even 10-fold more VRP_{3014} could not enhance protection of aged mice (data not shown).

Vaccination with a cocktail of divergent S-expressing VRPs does not enhance the quality or breadth of the immune response in aged mice. The development of an adequate neutralizing antibody response against the SARS S glycoprotein through vaccination is necessary to prevent SARS-CoV replication after challenge. We performed an ELISA with post-boost sera and varied the target antigen in order to gauge cross-reactivity of the immune response (Fig. 3C). When comparing peak IgG titers in each vaccine group expressing single S variants, the titer of the greatest magnitude was typically against the cognate vaccine antigen (Fig. 3C). Not surprisingly, the mean $\log_{10}$ half-maximal IgG responses within the pool-S group were similar for each antigen in the cocktail, with maximal IgG S responses to each S equivalent to those generated from the single-S-vaccinated groups (Fig. 3C). Importantly, sera from control VRP HA animals did not significantly cross-react with the SARS antigens, and the magnitudes of HA-specific responses were comparable to those seen in the SARS S groups (Fig. 3C). Although the degree of mortality varied

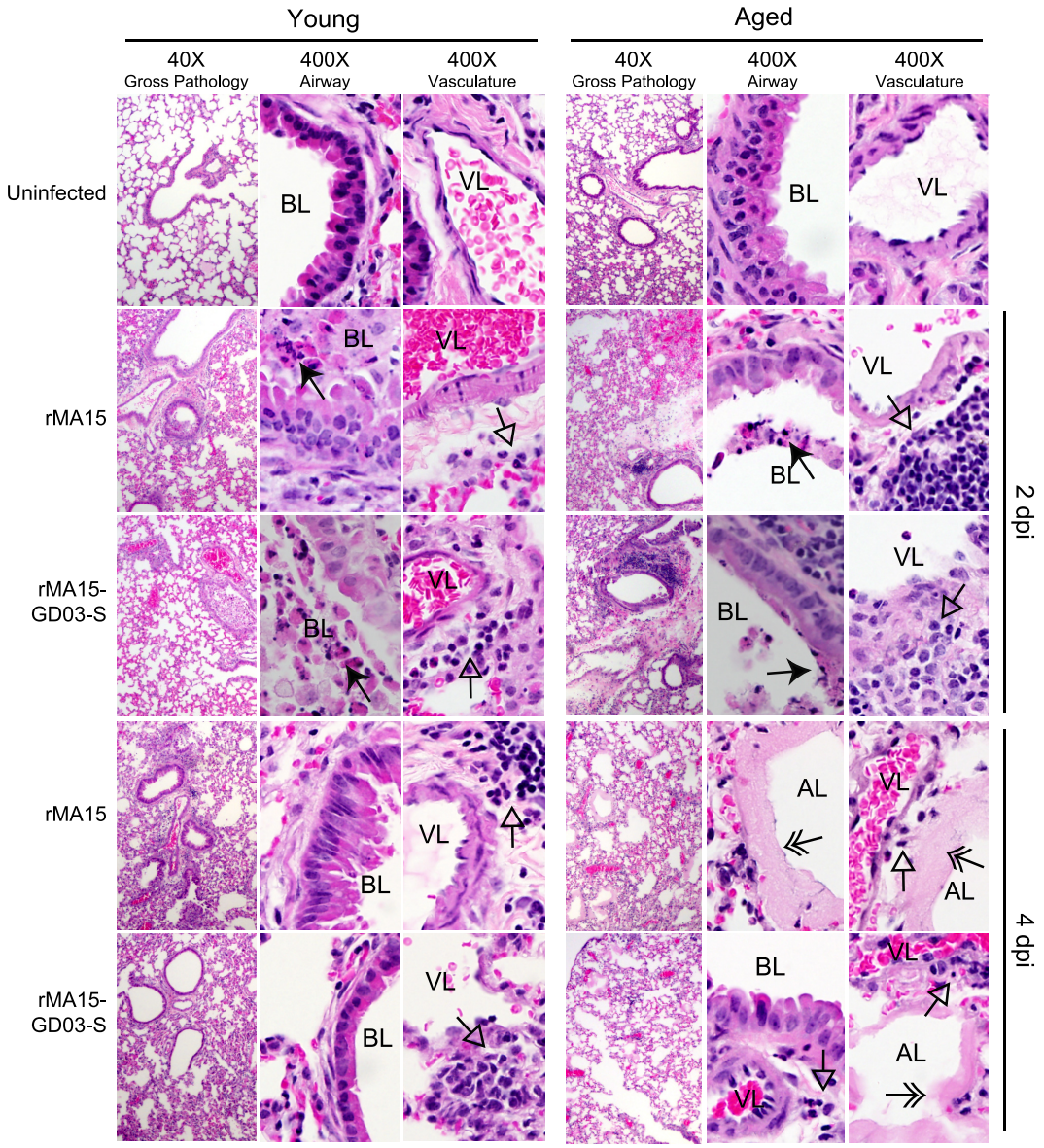

FIG. 2. rMA15 and rMA15 GD03-S infection induces ARDS in aged mice. Lung pathology of mock-infected and SARS-CoV-infected mice (2 and 4 dpi) was determined through blind scoring of H&E-stained lung sections. Compared to mock-infected animals, young animals infected with rMA15 or rMA15 GD03 experienced a denuding bronchiolitis with an accumulation of apoptotic debris within the airways (solid arrow) and perivascular cuffing caused predominately by lymphocytes (open arrowhead). Virus-induced lung pathology in the airways of aged mice was similar to that in young mice (filled arrowhead), while the peribronchivascular cuffing associated with infiltrating immune cells (open-headed arrow) was increased and readily visible at low power (dense purple areas; 40×). In contrast to results at 2 dpi, damage to the conducting airway (apoptotic debris in the airway, denuding bronchiolitis, etc.) was minimal and peribronchivascular cuffing (open arrowhead) was less severe at 4 dpi in both young and aged mice. Most importantly, hyaline membranes (double-headed arrow), a sign of diffuse alveolar damage and ARDS, were observed in many alveoli in aged animals infected with rMA15 or rMA15 GD03-S. These data suggest that the development of end-stage lung disease (ARDS) in SARS-infected animals is age related and that aged animals most likely die from ARDS, while the cause of death in young animals remains unknown. Vascular, alveolar, and bronchiolar lumen are labeled as VL, AL, and BL, respectively.

slightly between groups, the magnitudes of the mean $\log_{10}$ half-maximal GD03-specific IgG titers in each group were similar (Fig. 3C). Importantly, animals receiving 10^6 IU VRP_{3014} Urbani-S had significantly elevated half-maximal IgG titers (mean half-maximal Urbani IgG titer, 3.067 ± 0.258; P = 0.0020) compared to animals that received 10^5 IU, but this immune response was not robust enough to prevent morbidity or mortality (data not shown). We performed a microneutralization assay with rMA15 GD03-S to generate 50% neutralization titers from postboost sera for each animal in the study (Fig. 3D). One animal in the SZ16 group and one animal in the GD03 group had a reciprocal 50% neutralization titer of 25, while all other animals tested had titers below the limit of detection. These data demonstrate (i) the inclusion of various S antigens or a pool of S antigens does not increase the magnitude of IgG cross-reactivity in aged animals with this vaccine

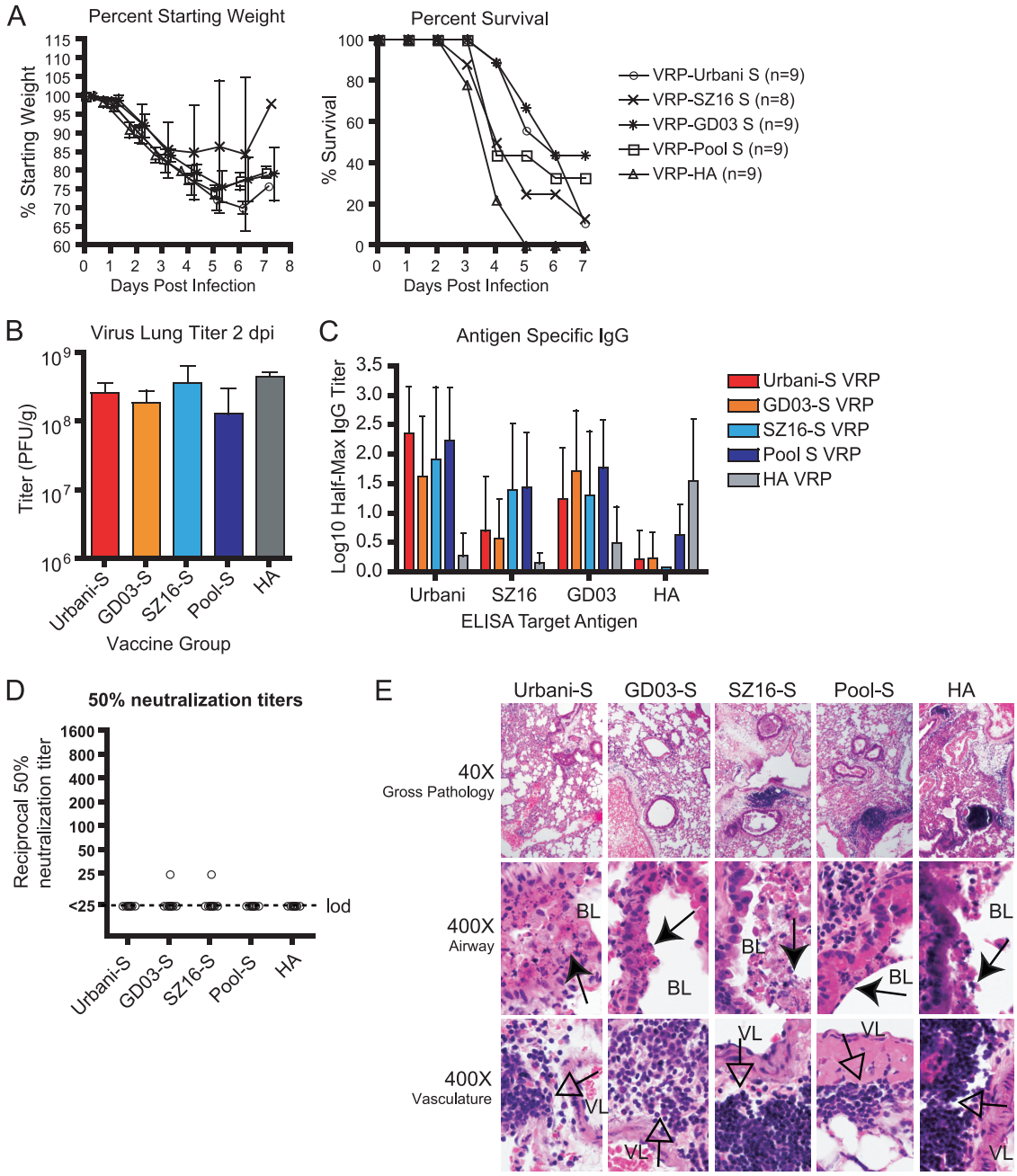

FIG. 3. Morbidity and mortality was seen in all experimental groups of VRP_{3014}-vaccinated 15-month-old rMA15 GD03-S-challenged BALB/c mice. Twelve-month-old Harlan Sprague Dawley mice (Indianapolis, IN) were vaccinated in a prime/boost regimen with 10^5 IU/10 μl of either VRP_{3014} HA, SARS-S, GD03-S, SZ16-S VRP, or a pool of SARS S containing VRPs (pool-S) in the left rear footpad. At 15 months of age, mice were infected with 10^5 PFU/50 μl rMA15 GD03-S. (A) Morbidity (weight loss) and mortality were monitored daily. Error bars represent 1 standard deviation. (B) Virus lung titers were assessed through standard plaque assay of clarified lung homogenates in Vero E6 cells, and average virus lung titers were similar in all vaccinated groups at 2 dpi. Error bars represent 1 standard deviation. (C) The antigen-specific IgG response was measured in postboost sera in triplicate by ELISA for each animal in which the Urbani-S, GD03-S, SZ16-S, or HA ELISA target antigen was employed, allowing for the assessment of cross-reactivity. Error bars represent 1 standard deviation. (D) The percent neutralization for postboost sera was determined in a microneutralization assay. Serum was serially diluted in 2-fold increments beginning at 1:25 and then mixed with 100 PFU of rMA15 GD03-S and incubated for 1 h at 37°C. Virus and sera was then added to a 96-well plate of Vero E6 cells (5×10^3 Vero E6 cells/well) in triplicate, and the development of CPE was scored 4 to 5 dpi. The greatest dilution of serum with more than two wells of protection was reported as the 50% neutralization titer. (E) Lung pathology at 2 dpi was determined through the blind scoring of H&E-stained lung sections. Peribronchivascular cuffing was evident in all groups at low magnification (40×). At high power, cuffing (opn arrowhead) was caused predominately by lymphocytes and neutrophils. Denuding bronchiolitis, focal apoptosis of the airway epithelium (filled arrowhead), and blockage of the airway with apoptotic debris (filled arrowhead) were evident in GD03- and pool-vaccinated animals, and these manifestations of disease were more prominent in Urbani-, SZ16-, and HA-vaccinated animals. Vascular and bronchiolar lumen are labeled as VL and BL, respectively.

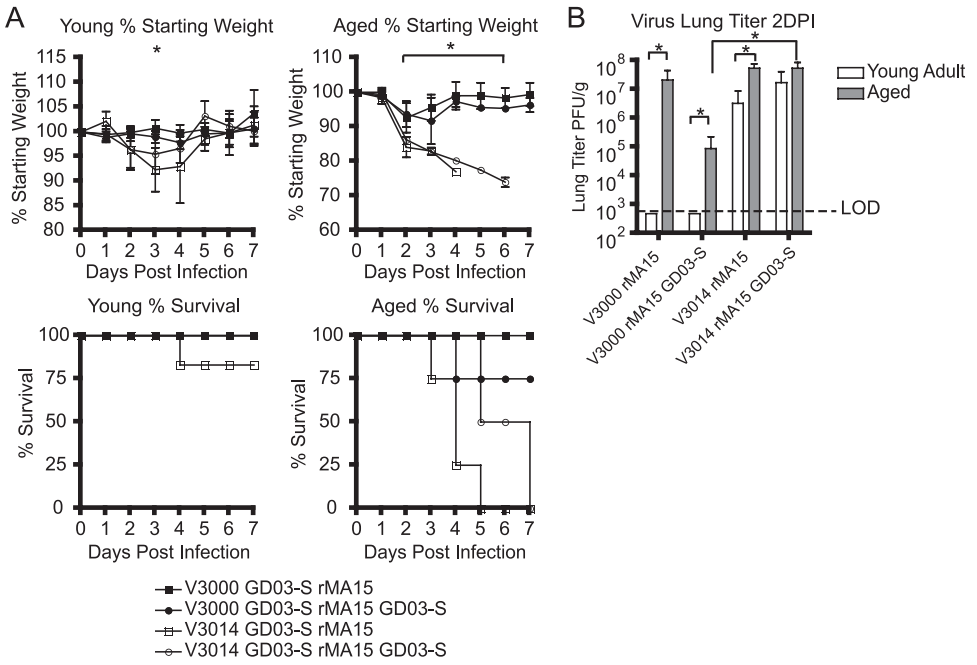

FIG. 4. Aged mice vaccinated with a wild-type VRP_{3000} vaccine expressing GD03-S are protected from SARS-CoV-induced mortality by both homologous and heterologous challenge. (A) Morbidity and mortality of young and aged animals vaccinated with VRP bearing the VEE 3014 or VEE 3000 glycoproteins expressing GD03-S in a prime/boost regimen and challenged with either rMA15 or rMA15 GD03-S. Error bars represent 1 standard deviation. (B) Virus titers were measured by plaque assay of clarified lung homogenates harvested at 2 dpi in Vero E6 cells. Significant differences ($P < 0.05$) between groups as judged by the Mann-Whitney test are marked with an asterisk. Error bars represent 1 standard deviation.

platform, (ii) VRP vaccination of aged mice with single S antigens or a pool of S antigens induces a robust antigen-specific IgG response, but the neutralizing antibody response is poor, leading to morbidity, mortality, and vaccine failure, and (iii) increasing the dose of VRP expressing Urbani-S to 10^6 IU in a prime/boost regimen significantly increased the antigen-specific serum IgG responses in aged animals compared to those receiving 10^5 IU, but this provided only partial protection from lethal heterologous challenge-induced morbidity and mortality.

Wild-type VRP vaccines protect both young and aged animals from lethal homologous and heterologous SARS-CoV challenge. Since VRP_{3014} vaccines failed to protect aged mice from virus-induced morbidity and mortality from a heterologous challenge, we hypothesized that (i) the aged immune system is incapable of developing a protective immune response through vaccination, and/or (ii) innate factors in the VRP_{3014} vaccine platform were contributing to vaccine failure in the aged.

To determine if VRP-dependent factors were influencing vaccine efficacy in the aged, we compared two different VRP vaccine platforms (VRP_{3014} and VRP_{3000}) in young and aged animals through lethal homologous/heterologous SARS-CoV challenge. VEE strain 3000 (wild-type) glycoproteins have been demonstrated to specifically target dendritic cells *in vivo*, and infection of mice with wild-type VEE 3000 is uniformly lethal (38). VEE strain 3014 glycoproteins contain three amino acid changes (E2, with E209K and I239N, and E1, with A272T) that completely attenuate VEE-induced mortality in mice, due at least in part to mutations that facilitate binding to heparan sulfate (E209K), altering *in vivo* cell tropism (7). Young (8 weeks) and aged (12 month) BALB/c mice were vaccinated in a prime/boost regimen with VRP_{3014} or VRP_{3000} expressing SARS-CoV GD03-S and were subsequently challenged with a lethal dose of rMA15 (heterologous) or rMA15 GD03-S (homologous). Upon challenge, young mice and aged mice were 14 weeks and 15 months old, respectively. In young adult mice, the VRP_{3000} GD03-S vaccine provided complete protection from morbidity, mortality, and virus replication (2 dpi) from both homologous and heterologous challenges, while the VRP_{3014} GD03-S-vaccinated groups experienced morbidity (mean percent weight loss nadir, 8% on 3 dpi), limited mortality (survival, 83%), and virus replication (Fig. 4A and B). Consistent with earlier experiments, VRP_{3014} GD03-S again failed to prevent morbidity and mortality in aged mice after heterologous challenge, but almost all VRP_{3000}-vaccinated mice were completely protected from clinical disease (Fig. 4A). While the VRP_{3000}-based vaccines failed to prevent virus replication upon challenge in aged mice, significant differences in virus lung titers were observed in comparison to VRP_{3014} (Fig. 4B). To assess lung pathology and inflammation postchallenge, H&E-stained lung sections from 2 dpi were blindly evaluated. Stark differences in lung pathology were seen when comparing sections from aged animals vaccinated with VRP_{3000} versus VRP_{3014} GD03-S (Fig. 5). In VRP_{3000} GD03-S-vaccinated and rMA15 GD03-S-challenged animals, the airway epithelium appeared normal and only minor peribronchivascular cuffing by lymphocytes was observed. Similarly, VRP_{3000} GD03-S vaccinated animals heterologously challenged with rMA15 displayed normal airway epithelium but moderate cuffing of airways and vasculature. In contrast, inflammation and damage to the airways were visible at low power in VRP_{3014} GD03-S-

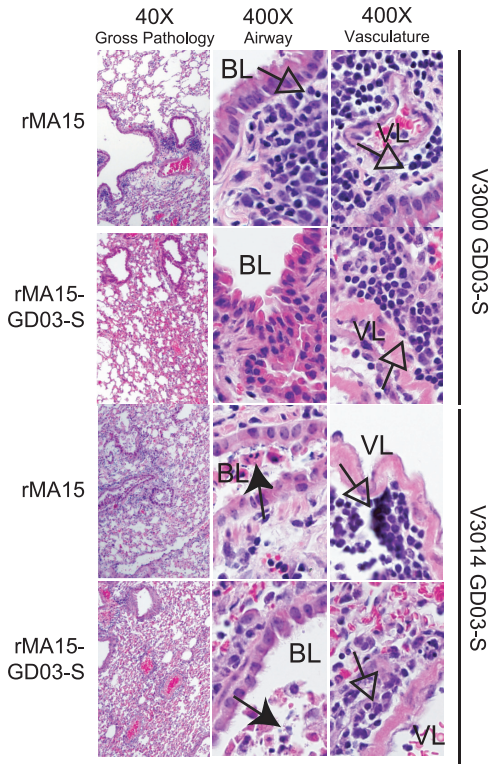

FIG. 5. Aged mice are protected from severe SARS-CoV-induced lung pathology through vaccination with variant VRPs. Lung pathology in VRP-vaccinated aged mice was evaluated in H&E-stained lung sections from 2 dpi in a blind manner. The airway epithelium appeared normal, and only minor peribronchivascular cuffing by lymphocytes was seen in animals receiving the V3000 GD03-S vaccine and homologously challenged with rMA15 GD03-S. Similarly, VRP_{3000} GD03-S-vaccinated mice heterologously challenged with rMA15 displayed normal airway epithelium but moderate cuffing of airways and vasculature. In contrast, inflammation and damage to the airways were visible at low power in VRP_{3014} GD03-S-vaccinated animals challenged with either rMA15 or rMA15 GD03-S. At high power (400×), denuding bronchiolitis, an accumulation of apoptotic debris in the airway (filled arrowhead), and moderate lymphocytic prebronchivascular cuffing (open arrowhead) was seen in VRP_{3014}-vaccinated and challenged animals.

vaccinated animals challenged with either rMA15 or rMA15 GD03-S, with denuding bronchiolitis, an accumulation of apoptotic debris in the airway, and moderate lymphocytitic prebronchivascular cuffing. The severe lung pathology seen in naïve animals infected with rMA15 and rMA15-GD03-S (Fig. 2, DAD/ARDS) was not observed in vaccinated animals.

Wild-type VRP vaccines protect young and aged animals from lethal homolgous influenza virus challenge. Since both SARS-CoV and influenza virus cause more severe disease in the aged, we broadened our scope to include influenza virus vaccine/lethal challenge studies that were similar in design to the SARS-CoV vaccine/challenge studies described above (5, 6). Young adult and aged mice were vaccinated with VRP_{3000} or VRP_{3014} expressing influenza virus HA in a prime/boost regimen. Similar to SARS-CoV-vaccinated and challenged young adult mice, VRP_{3000} HA vaccination was successful in preventing morbidity, mortality, and virus replication from lethal influenza virus PR8 challenge (Fig. 6A and B). VRP_{3014} HA vaccination protected young mice from disease but not from virus replication (Fig. 6A and B). Interestingly, the VRP_{3000} HA was successful in preventing morbidity, mortality, and PR8 virus replication in aged animals, while the VRP_{3014} HA vaccine provided only partial protection against disease and none against virus replication (Fig. 6A and B). All naïve young adult and unvaccinated aged mice uniformly succumbed to infection by 7 dpi (Fig. 6A). To assess lung pathology in vaccinated animals, H&E-stained lung sections from 3 dpi were blindly evaluated. In naive (mock-infected) young or in aged animals infected with influenza virus PR8, denuding bronchiolitis, apoptosis of airway epithelial cells, and an accumulation of apoptotic debris within the airway were observed, while peribronchivascular cuffing by lymphocytes and neutrophils was visible at low magnification (×40) (Fig. 7). Interestingly, young animals vaccinated with VRP_{3014} HA presented with similar pathology to naïve PR8-infected animals of the same age, while virus-induced lung pathology was minimal in the VRP_{3000} HA group. In aged HA-vaccinated animals, pathology within the airway epithelium and peribronchivascular cuffing were less severe than in young vaccinated animals, but striking differences between the vaccine groups VRP_{3000} HA and VRP_{3014} HA were not observed.

Antigen-specific serum IgG and neutralizing antibody responses are correlated with protection from disease and prevention of virus replication upon SARS-CoV or influenza virus challenge. Our previous experimentation suggested that VRP_{3014}-based vaccines can generate antigen-specific immune responses in aged animals but fail to generate sufficient protective neutralizing antibodies. We hypothesized that vaccine-specific factors or the aged immune system are responsible for the failure to generate an adequate protective immune response. To address this hypothesis, we performed several assays on postboost sera from young and aged VRP_{3000}- and VRP_{3014}-vaccinated animals as described above in the challenge studies (ELISA to measure antigen-specific IgG, a $PRNT_{50}$ assay using rMA15 GD03-S to measure amounts of SARS-CoV-neutralizing antibody, and an influenza virus HAI assay, whose titers are a known correlate of protection) (2). These data demonstrated that the aged immune system is quite capable of generating antigen-specific IgG responses comparable to those of young animals in groups receiving the VRP_{3000}-based vaccines (Fig. 8A). Moreover, groups that had limited morbidity and mortality (VRP_{3000}-vaccinated groups) had significantly greater antigen-specific IgG responses than groups that became ill (VRP_{3014}-vaccinated groups), suggesting that serum IgG responses correlate with protection from disease (Fig. 8A). Furthermore, serum neutralizing antibody titers in both VRP_{3000} GD03-S and HAI titers in HA-vaccinated groups were significantly higher than in the VRP_{3014} groups, demonstrating that the magnitudes of both neutralizing antibodies and HAI titers correlate with protection from disease and death in the aged (Fig. 8B and C). In order to ensure that the differences we had seen in the magnitude of the immune responses through the delivery of equivalent PFU was not due to the delivery of disparate numbers of total vaccine particles, we vaccinated young and aged mice with equivalent genomes of VRP_{3000} and VRP_{3014} expressing SARS-S. Similar to what we had seen previously, the SARS-S-specific IgG ELISA titers in VRP_{3000}-vaccinated young and aged animals

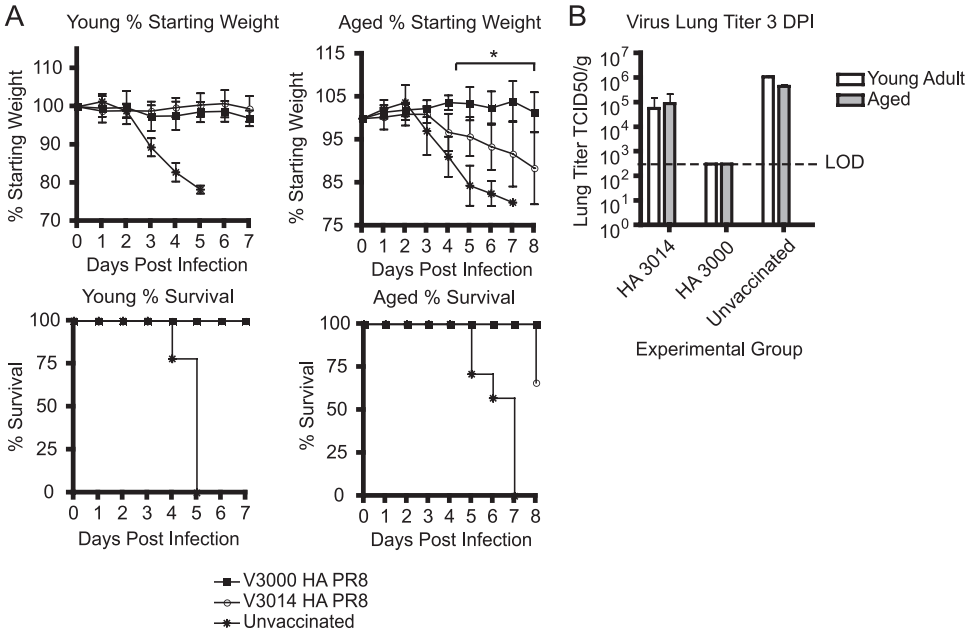

FIG. 6. Aged mice vaccinated with a wild-type VRP_{3000} expressing influenza virus HA are protected from lethal influenza virus challenge. (A) Morbidity and mortality of young and aged vaccinated or naïve mice were monitored after a lethal influenza virus PR8 infection (500 PFU). Significant differences ($P < 0.05$) between groups as judged by the Mann-Whitney test are marked with an asterisk. Error bars represent 1 standard deviation. (B) Virus replication was measured in clarified lung homogenates in a $TCID_{50}$ assay in MDCK cells. Error bars represent 1 standard deviation.

(young, 3.863 ± 0.064; aged, 2.689 ± 0.301) were significantly greater in magnitude (aged VRP_{3000} versus aged VRP_{3014}, $P = 0.0043$; young VRP_{3000} versus young VRP_{3014}, $P = 0.0022$) to those generated by VRP_{3014} vaccines (young, 2.106 ± 1.432; aged, 0.799 ± 1.084) (data not shown). Taken together, these data demonstrate that the aged immune system is capable of generating a robust protective immune response, given the appropriate stimulus, and VRP_{3000}-based vaccines induce significantly more robust immune responses in the young and aged compared to VRP_{3014}-based vaccines.

DISCUSSION

The dysregulation of the immune system with aging (i.e., immunosenescence) is in part responsible for the disproportionate rates of disease observed in the elderly infected with SARS-CoV, influenza virus, or West Nile virus and decreased efficacy of vaccination in the aged (1, 9, 25, 35, 43, 61). Furthermore, human infection by SARS-CoV and recently emerged influenza viruses (H5N1 and H1N1) can cause a most severe respiratory condition, ARDS, whose development resulting from SARS-CoV infection was a function of increasing age (28, 40, 45, 70). The molecular mechanisms responsible for age-related susceptibility to severe viral diseases and the potential overlap with mechanisms of age-related vaccine failures are not well understood. Surprisingly, very few small animal models exist to simultaneously study disproportionate viral disease in the aged and age-related defects for vaccine efficacy. Roberts et al. elegantly developed a mouse-adapted SARS-CoV (MA15) model through serial passage of SARS Urbani in the lungs of young BALB/c mice, but its pathogenesis in aged mice has not yet been reported (49). Using the novel rMA15 GD03-S SARS-CoV and its parent rMA15, we developed two models of SARS-CoV pathogenesis that mimicked the age-related severity of disease and age-related development of ARDS seen in humans during the recent SARS epidemic. Since young adult mice survive rMA15 GD03-S infection but aged mice do not, these data suggest that the Y436H mouse-adapting mutation, which was selected for function in the Urbani backbone, loses its potency in the context of the GD03-S structure. Importantly, the attenuating effects of GD03-S on pathogenesis in young mice are likely cancelled by age-related defects in the immune/pulmonary systems that contribute to the increased pathogenesis. Although mouse lung titer data for both rMA15 and rMA15 GD03-S were similar at the times evaluated (2 and 4 dpi), the *in vitro* growth data suggested that rMA15 may also hold a growth advantage prior to 2 dpi, likely setting the course for lethal infection. Most importantly, unlike young mice infected with rMA15, only rMA15-infected and rMA15 GD03-S-infected aged mice developed signs of ARDS, although all three infections were uniformly fatal. These data suggest that age-related host factors contribute to the development of ARDS and that the cause of death in young and aged mice infected with rMA15 are likely different. Although aged models of SARS-CoV pathogenesis and ARDS in C57BL/6 strains have not yet been reported, we recently demonstrated that rMA15 infection of young C57BL/6 mice results in survival, suggesting that host genetics as well as age play an integral role in the prevention or progression to ARDS (54). Furthermore, recent studies by Frieman et al. suggest that a host innate signaling protein, STAT1, contributes to the development of ARDS in mice infected with SARS-CoV, solidifying the hypothesis that both age and host factors contribute

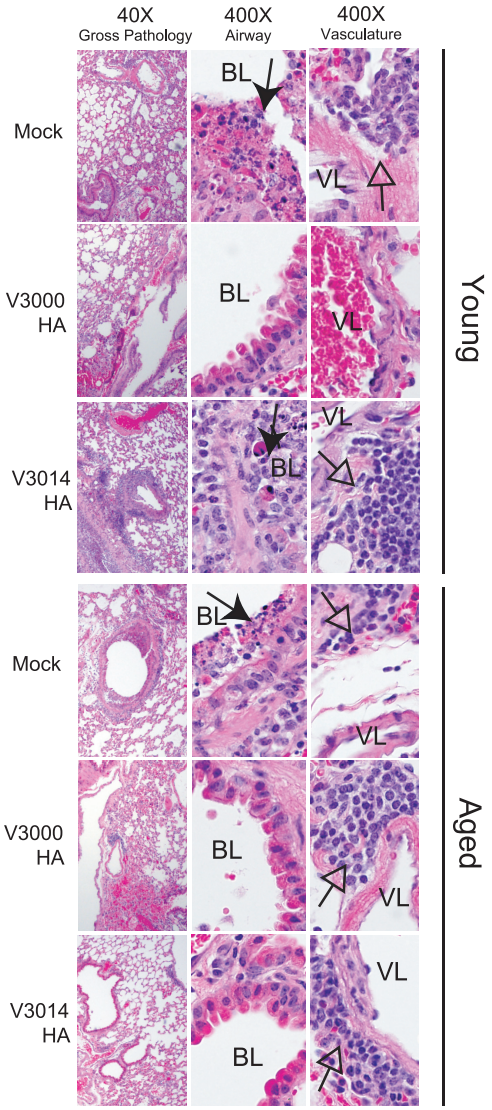

FIG. 7. Young and aged mice are protected from severe influenza virus-induced lung pathology through VRP vaccination. Lung pathology in naïve or VRP-vaccinated young and aged mice was evaluated in H&E-stained lung sections harvested at 3 dpi in a blind manner. In naive (mock) young or aged animals, denuding bronchiolitis, apoptosis of airway epithelial cells, and an accumulation of apoptotic debris within the airway was observed (filled arrowhead). Also, peribronchivascular cuffing (open arrowhead) visible at low power (40×) was observed, caused predominately by lymphocytes and neutrophils. In young vaccinated animals, VRP_{3014} HA-vaccinated animals presented with similar pathology to naïve PR8-infected animals, while virus-induced lung pathology was minimal in all of the VRP_{3000} HA-vaccinated groups. In aged vaccinated animals, pathology within the airway epithelium and peribronchivascular cuffing was less severe than in young vaccinated animals. The pathology seen in aged naïve animals was identical to that seen in young naïve animals.

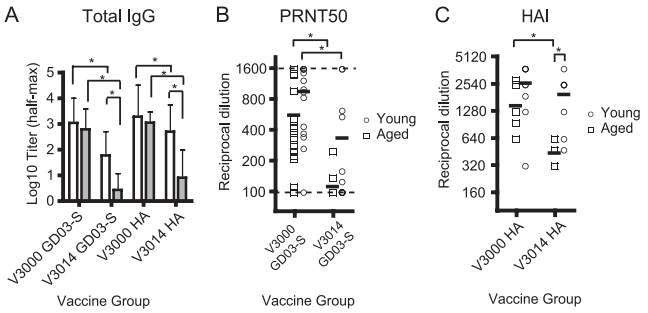

FIG. 8. The successful generation of a neutralizing antibody response in aged mice through VRP_{3000} vaccination correlates with protection from mortality. (A) Antigen-specific total IgG was measured in triplicate in postboost sera of young and aged mice vaccinated with VRP_{3000} GD03-S, V3014 GD03-S, VRP_{3000} HA, or VRP_{3014} HA. (B) The neutralizing antibody response was measured in GD03-S-vaccinated young and aged animals in a $PRNT_{50}$ assay, in which we report the serum dilution that reduced plaque numbers by 50%. (C) Influenza virus HA-specific antibody levels, a known correlate of protection, were measured in an HIA. Significant differences ($P < 0.05$) between groups as judged by the Mann-Whitney test are marked with an asterisk. Error bars represent 1 standard deviation.

to the development of end-stage lung disease resulting from virus infection (23). Interestingly, influenza virus strain A/PR8/34, which was adapted for lethal disease in young mice, does not produce more severe disease in aged animals, suggesting that tightly balanced virus-host interactions likely contribute to age-related disease. The development of small animal models with age-related influenza disease severity might provide a more relevant system for the evaluation of mechanisms of influenza virus pathogenesis and vaccine efficacy. The data from the rMA15/rMA15 GD03-S models suggest that (i) 1-year-old, aged animals are more susceptible to infection due to immunosenescence, (ii) one or more protective host responses within young adult mice are absent in aged mice, or that (iii) aged mice are less resilient in handling acute lung damage. We also recognize that a complex interplay of all three scenarios or yet-undiscovered scenarios could potentially explain the enhanced mortality and development of ARDS within aged animals as well.

Not only are effective multivalent platforms needed for vaccinating aged populations, but the choice of vaccine and antigen design for controlling emerging and reemerging pathogens further complicates an already difficult task due to the unknown antigenic identity of future emergents. Because surveillance and tracking of potential emerging viral diseases in wild animal populations is difficult and time-consuming, our most effective public health intervention may be to develop vaccine platforms that induce broadly cross-reactive immunity in all ages. Prior to this report, all SARS-CoV vaccine studies in mice were performed within SARS-CoV replication models for which modest viral loads were seen in the lung postinfection and overt signs of clinical disease were not observed (11, 15, 17, 18, 58, 67). Furthermore, vaccination and challenge of young adult mice, whose immune system is uncompromised, is not the most stringent evaluation of vaccine efficacy. Vaccine studies of the aged, who are in part immunocompromised, provide a much more stringent system to assess the robustness and efficacies of vaccines (15). Like SARS-CoV, few studies of influenza vaccine efficacy have been performed in aged mouse models, even though seasonal influenza affects the aged most severely. In 1993, Ben-Yehuda et al. demonstrated that a recombinant vaccinia virus vaccine expressing influenza virus PR8 HA protected aged mice from intranasal challenge by a homologous PR8 strain while conventional vaccines (killed

virus vaccine) failed (6). Similarly, Asanuma et al. (3) demonstrated partial protection of various strains (BALB/c, C57BL/6, and C3H) of aged mice from PR8 challenge after conventional vaccination (3). Since effective vaccination strategies in the elderly have not yet been developed for norovirus, influenza virus, West Nile virus, and SARS-CoV, the development of small animal models of age-related viral pathogenesis to study the efficacy of new vaccine platforms in aged populations could have a broad public health application. With this report, we demonstrate the effective VRP-based vaccination of aged populations through the generation of a robust cross-reactive immune response that facilitated protection from homologous and heterologous lethal SARS-CoV challenge and homologous lethal influenza virus challenge. As immune functions deteriorate with in aging, vaccine formulations that protect the aged will almost certainly be extremely successful in younger adults and may well be a universal paradigm regardless of vaccine design.

VRP vaccines have recently been clinically proven to be safe, replication-incompetent vaccine vectors capable of inducing mucosal immunity from a peripheral route of inoculation (8, 37, 60). Our current study confirms and expands upon earlier studies within SARS-CoV replication models in which the resultant immune responses from VRP_{3014} SARS-S vaccination in aged mice were insufficient to prevent heterologous challenge virus replication (15). Since the delivery of single VRP_{3014}-S, a pool of VRP_{3014}-S, and even 10-fold more VRP_{3014}-S failed to provide protection from lethal disease after heterologous challenge, we hypothesized that vaccine-specific factors and/or immunosenescence might be responsible for the failure of VRP_{3014}-based vaccines in the aged. To test this hypothesis, we constructed variant VRP vaccines packaged with either VEE strain 3014 glycoproteins, as used in previous experiments (Deming et al. and other studies described above) or wild-type VEE strain 3000 glycoproteins (15). Using VRP_{3000}-based vaccines, we demonstrated protection of the aged against two disparate respiratory viral infections that disproportionately affect the aged. The control of virus replication and the limited morbidity/mortality in the VRP_{3000} groups was coincident with the generation of a robust neutralizing antibody response consistent with several reports in which passive transfer of human monoclonal antibodies was highly protective against both lethal homologous and heterologous SARS-CoV (51, 52). Although the delivery of a cocktail of VRP_{3014}-based vaccines failed to enhance cross-protection and survival, it will be interesting to assess the potential enhancement of the immune response by cocktails of VRP_{3000}-based vaccines in protection from lethal heterologous SARS-CoV strains. Furthermore, given the recent data of Wei et al., who reported a DNA prime/adenovirus 5 boost vaccine regimen enhanced cross-neutralization of divergent influenza virus strains over the traditional influenza vaccine, it will be interesting to see if the immune response generated by VRP_{3000}-based influenza vaccines will protect against heterologous influenza virus challenge (65). Future studies comparing VRP_{3000} and VRP_{3014} may help elucidate novel molecular immunologic defects related to immunosenescence and at the least identify the immunologic signatures required for VRP-mediated protection in the aged. Moreover, our data suggest that VRP coats and/or dosages may need to be altered for use in elderly populations in order to provide protection from diseases that cause disproportionate disease in the aged.

Studies of VEE pathogenesis and recent VRP vaccine studies help explain the differences seen when comparing the immune responses generated by VRP_{3000} and VRP_{3014}. Data from Bernard et al. and Macdonald et al. suggest that VEE_{3014} glycoproteins (amino acid changes from wild-type VEE_{3000}, E2 with E209K and I239N and E1 with A272T) nonspecifically bind heparan sulfate on the surface of cultured cells and the natural *in vivo* cell targeting of dendritic cells is abrogated by heparan sulfate-binding mutations (7, 38). In support of the VEE studies discussed above, Fluet et al. demonstrated that differential *in vivo* cell targeting by VRP_{3014} and VRP_{3000} significantly affected both cellular and humoral responses, where the VRP_{3000}-based vaccines induced superior immune responses in young adult mice (22). It is important to note that in comparing numbers of VRP genomes by real-time PCR and VRP "infectious unit" titers for BHK cells, Fluet et al. reported that VRP_{3000} is about 10- to 50-fold less infectious than VRP_{3014} *in vitro* (22). In effect, the vaccination of mice with similar numbers of infections units of VRP_{3000} or VRP_{3014} resulted in the delivery of approximately 10- to 50-fold more genome copies with VRP_{3000} vaccines, but vaccination with approximately 100-fold less VRP_{3000} resulted in an unchanged immune response still superior to that of the VRP_{3014} variant vaccine (22). Since an increased dose of VRP_{3000} vaccine did not increase the magnitude of the immune response accordingly, these data suggest that VRP_{3000} target cells *in vivo* are limiting and saturated even with a 100-fold reduction in dose. Similar to the findings of Fluet et al., we found that that delivery of equivalent genomes of VRP_{3014} or VRP_{3014} vaccines expressing SARS-S resulted in a significantly more robust immune response in VRP_{3000}-vaccinated animals, and this difference was evident in young and aged animals (22). Moreover, the delivery of 10-fold more IU of VRP_{3014} vaccine did not protect aged animals from lethal SARS-CoV challenge. Taken together, these results predict that repeated boosts with a VRP_{3014}-based vaccine would have minimal impact on improving immune responses in the aged due to altered *in vivo* targeting but that repeated doses of VRP_{3000}-based vaccines would generate enhanced responses based on the cells targeted and potential differences in the pathways of target cell antigen presentation. Future studies comparing immune cell targeting and dendritic cell activation and function as well as direct and indirect antigen presentation in young and aged vaccinated mice should help elucidate the molecular basis for VRP_{3000}'s superior immunogenic properties compared to VRP_{3014}.

Effective vaccines directed against emerging pathogens should induce the broadest possible immune response in order to maximize the probability that the vaccine will protect against future emergents from the zoonotic pool. Whenever possible, homologous vaccine challenge models without morbidity or mortality should be replaced by more stringent heterologous lethal challenge models, in order to more accurately model vaccine challenge by an emerging disease. Within our models of age-related SARS-CoV pathogenesis and ARDS, we have demonstrate the first effective vaccines in the aged that are sufficient to protect against heterologous lethal SARS-CoV challenge and lethal homologous influenza virus challenge. To build upon the data we have obtained in young and aged

mouse models, aged ferret and primate models should also be developed to expand the numbers of models within which scientists can study immunosenescence in the context of virus infection and vaccination. Compared to young animals, aged macaques display more severe disease pathology following SARS-CoV infection, potentially providing a robust nonhuman primate model for vaccine testing in aged populations (57). To our knowledge, similar models for influenza virus have not been reported. Finally, to maximize the public health benefits of vaccination, vaccine platform technologies should be successful for all ages and especially in the most vulnerable populations, like the elderly, who are often disproportionately targeted by emerging viral diseases such as SARS-CoV, West Nile virus, and influenza virus.

ACKNOWLEDGMENTS

We thank Peter Palese at Mount Sinai Medical Center for generously providing the recombinant influenza PR8 virus. We also thank Damon Deming and Boyd Yount for helpful discussions throughout these studies.

This work was supported by research grant PO1 AI59443 to R.S.B., R.E.J., and M.T.H. and by SERCEB U54 AI057157 from the National Institutes of Health, National Institute of Allergy and Infectious Diseases.

REFERENCES

1. **Anonymous.** 1995. From the Centers for Disease Control and Prevention. Pneumonia and influenza death rates—United States, 1979–1994. JAMA **274:**532.
2. **Anonymous.** 2009. Serum cross-reactive antibody response to a novel influenza A (H1N1) virus after vaccination with seasonal influenza vaccine. MMWR Morb. Mortal. Wkly. Rep. **58:**521–524.
3. **Asanuma, H., K. Hirokawa, M. Uchiyama, Y. Suzuki, C. Aizawa, T. Kurata, T. Sata, and S. Tamura.** 2001. Immune responses and protection in different strains of aged mice immunized intranasally with an adjuvant-combined influenza vaccine. Vaccine **19:**3981–3989.
4. **Baric, R. S., T. Sheahan, D. Deming, E. Donaldson, B. Yount, A. C. Sims, R. S. Roberts, M. Frieman, and B. Rockx.** 2006. SARS coronavirus vaccine development. Adv. Exp. Med. Biol. **581:**553–560.
5. **Bender, B. S., S. F. Taylor, D. S. Zander, and R. Cottey.** 1995. Pulmonary immune response of young and aged mice after influenza challenge. J. Lab. Clin. Med. **126:**169–177.
6. **Ben-Yehuda, A., D. Ehleiter, A. R. Hu, and M. E. Weksler.** 1993. Recombinant vaccinia virus expressing the PR/8 influenza hemagglutinin gene overcomes the impaired immune response and increased susceptibility of old mice to influenza infection. J. Infect. Dis. **168:**352–357.
7. **Bernard, K. A., W. B. Klimstra, and R. E. Johnston.** 2000. Mutations in the E2 glycoprotein of Venezuelan equine encephalitis virus confer heparan sulfate interaction, low morbidity, and rapid clearance from blood of mice. Virology **276:**93–103.
8. **Bernstein, D. I., E. A. Reap, K. Katen, A. Watson, K. Smith, P. Norberg, R. A. Olmsted, A. Hoeper, J. Morris, S. Negri, M. F. Maughan, and J. D. Chulay.** 2009. Randomized, double-blind, phase 1 trial of an alphavirus replicon vaccine for cytomegalovirus in CMV seronegative adult volunteers. Vaccine **28:**484–493.
9. **Bernstein, E., D. Kaye, E. Abrutyn, P. Gross, M. Dorfman, and D. M. Murasko.** 1999. Immune response to influenza vaccination in a large healthy elderly population. Vaccine **17:**82–94.
10. **Bernstein, E. D., E. M. Gardner, E. Abrutyn, P. Gross, and D. M. Murasko.** 1998. Cytokine production after influenza vaccination in a healthy elderly population. Vaccine **16:**1722–1731.
11. **Bisht, H., A. Roberts, L. Vogel, A. Bukreyev, P. L. Collins, B. R. Murphy, K. Subbarao, and B. Moss.** 2004. Severe acute respiratory syndrome coronavirus spike protein expressed by attenuated vaccinia virus protectively immunizes mice. Proc. Natl. Acad. Sci. U. S. A. **101:**6641–6646.
12. **Booth, C. M., L. M. Matukas, G. A. Tomlinson, A. R. Rachlis, D. B. Rose, H. A. Dwosh, S. L. Walmsley, T. Mazzulli, M. Avendano, P. Derkach, I. E. Ephtimios, I. Kitai, B. D. Mederski, S. B. Shadowitz, W. L. Gold, L. A. Hawryluck, E. Rea, J. S. Chenkin, D. W. Cescon, S. M. Poutanen, and A. S. Detsky.** 2003. Clinical features and short-term outcomes of 144 patients with SARS in the greater Toronto area. JAMA **289:**2801–2809.
13. **Chinese, S. M. E. C.** 2004. Molecular evolution of the SARS coronavirus during the course of the SARS epidemic in China. Science **303:**1666–1669.
14. **Davis, N. L., N. Powell, G. F. Greenwald, L. V. Willis, B. J. Johnson, J. F. Smith, and R. E. Johnston.** 1991. Attenuating mutations in the E2 glycoprotein gene of Venezuelan equine encephalitis virus: construction of single and multiple mutants in a full-length cDNA clone. Virology **183:**20–31.
15. **Deming, D., T. Sheahan, M. Heise, B. Yount, N. Davis, A. Sims, M. Suthar, J. Harkema, A. Whitmore, R. Pickles, A. West, E. Donaldson, K. Curtis, R. Johnston, and R. Baric.** 2006. Vaccine efficacy in senescent mice challenged with recombinant SARS-CoV bearing epidemic and zoonotic spike variants. PLoS Med. **3:**e525.
16. **Donnelly, C. A., A. C. Ghani, G. M. Leung, A. J. Hedley, C. Fraser, S. Riley, L. J. Abu-Raddad, L. M. Ho, T. Q. Thach, P. Chau, K. P. Chan, T. H. Lam, L. Y. Tse, T. Tsang, S. H. Liu, J. H. Kong, E. M. Lau, N. M. Ferguson, and R. M. Anderson.** 2003. Epidemiological determinants of spread of causal agent of severe acute respiratory syndrome in Hong Kong. Lancet **361:**1761–1766.
17. **Du, L., G. Zhao, Y. He, Y. Guo, B. J. Zheng, S. Jiang, and Y. Zhou.** 2007. Receptor-binding domain of SARS-CoV spike protein induces long-term protective immunity in an animal model. Vaccine **25:**2832–2838.
18. **Du, L., G. Zhao, Y. Lin, C. Chan, Y. He, S. Jiang, C. Wu, D. Y. Jin, K. Y. Yuen, Y. Zhou, and B. J. Zheng.** 2008. Priming with rAAV encoding RBD of SARS-CoV S protein and boosting with RBD-specific peptides for T cell epitopes elevated humoral and cellular immune responses against SARS-CoV infection. Vaccine **26:**1644–1651.
19. **Eaton, S. M., E. M. Burns, K. Kusser, T. D. Randall, and L. Haynes.** 2004. Age-related defects in CD4 T cell cognate helper function lead to reductions in humoral responses. J. Exp. Med. **200:**1613–1622.
20. **Edelson, B. T., and E. R. Unanue.** 2002. MyD88-dependent but Toll-like receptor 2-independent innate immunity to Listeria: no role for either in macrophage listericidal activity. J. Immunol. **169:**3869–3875.
21. **Effros, R. B.** 2007. Role of T lymphocyte replicative senescence in vaccine efficacy. Vaccine **25:**599–604.
22. **Fluet, M. E., A. C. Whitmore, D. A. Moshkoff, K. Fu, Y. Tang, M. L. Collier, A. West, D. T. Moore, R. Swanstrom, R. E. Johnston, and N. L. Davis.** 2008. Effects of rapid antigen degradation and VEE glycoprotein specificity on immune responses induced by a VEE replicon vaccine. Virology **370:**22–32.
23. **Frieman, M. B., J. Chen, T. E. Morrison, A. Whitmore, W. Funkhouser, J. M. Ward, E. W. Lamirande, A. Roberts, M. Heise, K. Subbarao, and R. S. Baric.** 2010. SARS-CoV pathogenesis is regulated by a STAT1 dependent but a type I, II and III interferon receptor independent mechanism. PLoS Pathog. **6:**e1000849.
24. **Fujihashi, K., T. Koga, and J. R. McGhee.** 2000. Mucosal vaccination and immune responses in the elderly. Vaccine **18:**1675–1680.
25. **Goodwin, K., C. Viboud, and L. Simonsen.** 2006. Antibody response to influenza vaccination in the elderly: a quantitative review. Vaccine **24:**1159–1169.
26. **Goronzy, J. J., J. W. Fulbright, C. S. Crowson, G. A. Poland, W. M. O'Fallon, and C. M. Weyand.** 2001. Value of immunological markers in predicting responsiveness to influenza vaccination in elderly individuals. J. Virol. **75:**12182–12187.
27. **Gruver, A. L., L. L. Hudson, and G. D. Sempowski.** 2007. Immunosenescence of ageing. J. Pathol. **211:**144–156.
28. **Guan, Y., B. J. Zheng, Y. Q. He, X. L. Liu, Z. X. Zhuang, C. L. Cheung, S. W. Luo, P. H. Li, L. J. Zhang, Y. J. Guan, K. M. Butt, K. L. Wong, K. W. Chan, W. Lim, K. F. Shortridge, K. Y. Yuen, J. S. Peiris, and L. L. Poon.** 2003. Isolation and characterization of viruses related to the SARS coronavirus from animals in southern China. Science **302:**276–278.
29. **Han, Y., H. Geng, W. Feng, X. Tang, A. Ou, Y. Lao, Y. Xu, H. Lin, H. Liu, and Y. Li.** 2003. A follow-up study of 69 discharged SARS patients. J. Tradit. Chin. Med. **23:**214–217.
30. **Hancock, K., V. Veguilla, X. Lu, W. Zhong, E. N. Butler, H. Sun, F. Liu, L. Dong, J. R. DeVos, P. M. Gargiullo, T. L. Brammer, N. J. Cox, T. M. Tumpey, and J. M. Katz.** 2009. Cross-reactive antibody responses to the 2009 pandemic H1N1 influenza virus. N. Engl. J. Med. **361:**1945–1952.
31. **Haynes, L., and S. L. Swain.** 2006. Why aging T cells fail: implications for vaccination. Immunity **24:**663–666.
32. **Hu, M. C., T. Jones, R. T. Kenney, D. L. Barnard, D. S. Burt, and G. H. Lowell.** 2007. Intranasal Protollin-formulated recombinant SARS S-protein elicits respiratory and serum neutralizing antibodies and protection in mice. Vaccine **25:**6334–6340.
33. **Lau, S. K., P. C. Woo, K. S. Li, Y. Huang, H. W. Tsoi, B. H. Wong, S. S. Wong, S. Y. Leung, K. H. Chan, and K. Y. Yuen.** 2005. Severe acute respiratory syndrome coronavirus-like virus in Chinese horseshoe bats. Proc. Natl. Acad. Sci. U. S. A. **102:**14040–14045.
34. **Lee, N., D. Hui, A. Wu, P. Chan, P. Cameron, G. M. Joynt, A. Ahuja, M. Y. Yung, C. B. Leung, K. F. To, S. F. Lui, C. C. Szeto, S. Chung, and J. J. Sung.** 2003. A major outbreak of severe acute respiratory syndrome in Hong Kong. N. Engl. J. Med. **348:**1986–1994.
35. **Leung, G. M., A. J. Hedley, L. M. Ho, P. Chau, I. O. Wong, T. Q. Thach, A. C. Ghani, C. A. Donnelly, C. Fraser, S. Riley, N. M. Ferguson, R. M. Anderson, T. Tsang, P. Y. Leung, V. Wong, J. C. Chan, E. Tsui, S. V. Lo, and T. H. Lam.** 2004. The epidemiology of severe acute respiratory syndrome in the 2003 Hong Kong epidemic: an analysis of all 1755 patients. Ann. Intern. Med. **141:**662–673.

36. **Liang, W., Z. Zhu, J. Guo, Z. Liu, W. Zhou, D. P. Chin, and A. Schuchat.** 2004. Severe acute respiratory syndrome, Beijing, 2003. Emerg. Infect. Dis. **10:**25–31.
37. **LoBue, A. D., L. Lindesmith, B. Yount, P. R. Harrington, J. M. Thompson, R. E. Johnston, C. L. Moe, and R. S. Baric.** 2006. Multivalent norovirus vaccines induce strong mucosal and systemic blocking antibodies against multiple strains. Vaccine **24:**5220–5234.
38. **MacDonald, G. H., and R. E. Johnston.** 2000. Role of dendritic cell targeting in Venezuelan equine encephalitis virus pathogenesis. J. Virol. **74:**914–922.
39. **McElhaney, J. E., J. W. Hooton, N. Hooton, and R. C. Bleackley.** 2005. Comparison of single versus booster dose of influenza vaccination on humoral and cellular immune responses in older adults. Vaccine **23:**3294–3300.
40. **Miller, R. R., III, B. A. Markewitz, R. T. Rolfs, S. M. Brown, K. K. Dascomb, C. K. Grissom, M. D. Friedrichs, J. Mayer, E. L. Hirshberg, J. Conklin, R. Paine III, and N. C. Dean.** 2009. Clinical findings and demographic factors associated with intensive care unit admission in Utah due to 2009 novel influenza A (H1N1) infection. Chest **139:**752–758.
41. **Monto, A. S., and R. J. Whitley.** 2008. Seasonal and pandemic influenza: a 2007 update on challenges and solutions. Clin. Infect. Dis. **46:**1024–1031.
42. **Morens, D. M., G. K. Folkers, and A. S. Fauci.** 2004. The challenge of emerging and re-emerging infectious diseases. Nature **430:**242–249.
43. **Murray, K., S. Baraniuk, M. Resnick, R. Arafat, C. Kilborn, K. Cain, R. Shallenberger, T. L. York, D. Martinez, J. S. Hellums, D. Hellums, M. Malkoff, N. Elgawley, W. McNeely, S. A. Khuwaja, and R. B. Tesh.** 2006. Risk factors for encephalitis and death from West Nile virus infection. Epidemiol. Infect. **134:**1325–1332.
44. **Pawelec, G., and A. Larbi.** 2008. Immunity and ageing in man: annual review 2006/2007. Exp. Gerontol. **43:**34–38.
45. **Peiris, J. S., C. M. Chu, V. C. Cheng, K. S. Chan, I. F. Hung, L. L. Poon, K. I. Law, B. S. Tang, T. Y. Hon, C. S. Chan, K. H. Chan, J. S. Ng, B. J. Zheng, W. L. Ng, R. W. Lai, Y. Guan, and K. Y. Yuen.** 2003. Clinical progression and viral load in a community outbreak of coronavirus-associated SARS pneumonia: a prospective study. Lancet **361:**1767–1772.
46. **Peiris, J. S., K. Y. Yuen, A. D. Osterhaus, and K. Stohr.** 2003. The severe acute respiratory syndrome. N. Engl. J. Med. **349:**2431–2441.
47. **Pushko, P., M. Parker, G. V. Ludwig, N. L. Davis, R. E. Johnston, and J. F. Smith.** 1997. Replicon-helper systems from attenuated Venezuelan equine encephalitis virus: expression of heterologous genes in vitro and immunization against heterologous pathogens in vivo. Virology **239:**389–401.
48. **Rimmelzwaan, G. F., M. Baars, E. C. Claas, and A. D. Osterhaus.** 1998. Comparison of RNA hybridization, hemagglutination assay, titration of infectious virus and immunofluorescence as methods for monitoring influenza virus replication in vitro. J. Virol. Methods **74:**57–66.
49. **Roberts, A., D. Deming, C. D. Paddock, A. Cheng, B. Yount, L. Vogel, B. D. Herman, T. Sheahan, M. Heise, G. L. Genrich, S. R. Zaki, R. Baric, and K. Subbarao.** 2007. A mouse-adapted SARS-coronavirus causes disease and mortality in BALB/c mice. PLoS Pathog. **3:**e5.
50. **Roberts, A., and K. Subbarao.** 2006. Animal models for SARS. Adv. Exp. Med. Biol. **581:**463–471.
51. **Rockx, B., D. Corti, E. Donaldson, T. Sheahan, K. Stadler, A. Lanzavecchia, and R. Baric.** 2008. Structural basis for potent cross-neutralizing human monoclonal antibody protection against lethal human and zoonotic severe acute respiratory syndrome coronavirus challenge. J. Virol. **82:**3220–3235.
52. **Rockx, B., T. Sheahan, E. Donaldson, J. Harkema, A. Sims, M. Heise, R. Pickles, M. Cameron, D. Kelvin, and R. Baric.** 2007. Synthetic reconstruction of zoonotic and early human severe acute respiratory syndrome coronavirus isolates that produce fatal disease in aged mice. J. Virol. **81:**7410–7423.
53. **Sheahan, T., D. Deming, E. Donaldson, R. Pickles, and R. Baric.** 2006. Resurrection of an "extinct" SARS-CoV isolate GD03 from late 2003. Adv. Exp. Med. Biol. **581:**547–550.
54. **Sheahan, T., T. E. Morrison, W. Funkhouser, S. Uematsu, S. Akira, R. S. Baric, and M. T. Heise.** 2008. MyD88 is required for protection from lethal infection with a mouse-adapted SARS-CoV. PLoS Pathog. **4:**e1000240.
55. **Sheahan, T., B. Rockx, E. Donaldson, D. Corti, and R. Baric.** 2008. Pathways of cross-species transmission of synthetically reconstructed zoonotic severe acute respiratory syndrome coronavirus. J. Virol. **82:**8721–8732.
56. **Sheahan, T., B. Rockx, E. Donaldson, A. Sims, R. Pickles, D. Corti, and R. Baric.** 2008. Mechanisms of zoonotic severe acute respiratory syndrome coronavirus host range expansion in human airway epithelium. J. Virol. **82:**2274–2285.
57. **Smits, S. L., A. de Lang, J. M. van den Brand, L. M. Leijten, I. W. F. van, M. J. Eijkemans, G. van Amerongen, T. Kuiken, A. C. Andeweg, A. D. Osterhaus, and B. L. Haagmans.** 2010. Exacerbated innate host response to SARS-CoV in aged non-human primates. PLoS Pathog. **6:**e1000756.
58. **Spruth, M., O. Kistner, H. Savidis-Dacho, E. Hitter, B. Crowe, M. Gerencer, P. Bruhl, L. Grillberger, M. Reiter, C. Tauer, W. Mundt, and P. N. Barrett.** 2006. A double-inactivated whole virus candidate SARS coronavirus vaccine stimulates neutralising and protective antibody responses. Vaccine **24:**652–661.
59. **Subbarao, K., J. McAuliffe, L. Vogel, G. Fahle, S. Fischer, K. Tatti, M. Packard, W. J. Shieh, S. Zaki, and B. Murphy.** 2004. Prior infection and passive transfer of neutralizing antibody prevent replication of severe acute respiratory syndrome coronavirus in the respiratory tract of mice. J. Virol. **78:**3572–3577.
60. **Thompson, J. M., A. C. Whitmore, J. L. Konopka, M. L. Collier, E. M. Richmond, N. L. Davis, H. F. Staats, and R. E. Johnston.** 2006. Mucosal and systemic adjuvant activity of alphavirus replicon particles. Proc. Natl. Acad. Sci. U. S. A. **103:**3722–3727.
61. **Thompson, W. W., D. K. Shay, E. Weintraub, L. Brammer, N. Cox, L. J. Anderson, and K. Fukuda.** 2003. Mortality associated with influenza and respiratory syncytial virus in the United States. JAMA **289:**179–186.
62. **Vallejo, A. N.** 2005. CD28 extinction in human T cells: altered functions and the program of T-cell senescence. Immunol. Rev. **205:**158–169.
63. **Vasto, S., M. Malavolta, and G. Pawelec.** 2006. Age and immunity. Immun. Ageing **3:**2.
64. **Wang, C. Q., K. B. Udupa, H. Xiao, and D. A. Lipschitz.** 1995. Effect of age on marrow macrophage number and function. Aging (Milano) **7:**379–384.
65. **Wei, C. J., J. C. Boyington, P. M. McTamney, W. P. Kong, M. B. Pearce, L. Xu, H. Andersen, S. Rao, T. M. Tumpey, Z. Y. Yang, and G. J. Nabel.** 2010. Induction of broadly neutralizing H1N1 influenza antibodies by vaccination. Science **329:**1060–1064.
66. **Wen, Z., L. Ye, Y. Gao, L. Pan, K. Dong, Z. Bu, R. W. Compans, and C. Yang.** 2009. Immunization by influenza virus-like particles protects aged mice against lethal influenza virus challenge. Antiviral Res. **84:**215–224.
67. **Yang, Z. Y., W. P. Kong, Y. Huang, A. Roberts, B. R. Murphy, K. Subbarao, and G. J. Nabel.** 2004. A DNA vaccine induces SARS coronavirus neutralization and protective immunity in mice. Nature **428:**561–564.
68. **Yount, B., K. M. Curtis, E. A. Fritz, L. E. Hensley, P. B. Jahrling, E. Prentice, M. R. Denison, T. W. Geisbert, and R. S. Baric.** 2003. Reverse genetics with a full-length infectious cDNA of severe acute respiratory syndrome coronavirus. Proc. Natl. Acad. Sci. U. S. A. **100:**12995–13000.
69. **Yount, B., R. S. Roberts, A. C. Sims, D. Deming, M. B. Frieman, J. Sparks, M. R. Denison, N. Davis, and R. S. Baric.** 2005. Severe acute respiratory syndrome coronavirus group-specific open reading frames encode nonessential functions for replication in cell cultures and mice. J. Virol. **79:**14909–14922.
70. **Yu, H., Z. Gao, Z. Feng, Y. Shu, N. Xiang, L. Zhou, Y. Huai, L. Feng, Z. Peng, Z. Li, C. Xu, J. Li, C. Hu, Q. Li, X. Xu, X. Liu, Z. Liu, L. Xu, Y. Chen, H. Luo, L. Wei, X. Zhang, J. Xin, J. Guo, Q. Wang, Z. Yuan, K. Zhang, W. Zhang, J. Yang, X. Zhong, S. Xia, L. Li, J. Cheng, E. Ma, P. He, S. S. Lee, Y. Wang, T. M. Uyeki, and W. Yang.** 2008. Clinical characteristics of 26 human cases of highly pathogenic avian influenza A (H5N1) virus infection in China. PLoS One **3:**e2985.